

ALASCA: Rethinking Label Smoothing for Deep Learning Under Label Noise

Jongwoo Ko¹ Bongsoo Yi² Se-Young Yun¹

Abstract

As label noise, one of the most popular distribution shifts, severely degrades deep neural networks' generalization performance, robust training with noisy labels is becoming an important task in modern deep learning. In this paper, we propose our framework, coined as Adaptive Label smoothing on Sub-Classifier (ALASCA), that provides a robust feature extractor with theoretical guarantee and negligible additional computation. First, we derive that the label smoothing (LS) incurs implicit Lipschitz regularization (LR). Furthermore, based on these derivations, we apply the adaptive LS (ALS) on sub-classifiers architectures for the practical application of adaptive LR on intermediate layers. We conduct extensive experiments for ALASCA and combine it with previous noise-robust methods on several datasets and show our framework consistently outperforms corresponding baselines.

1. Introduction

Modern deep neural networks (DNNs) have expressive power and high capacity, resulting in accurate modeling and promising generalization. However, a big challenge in the age of deep learning is distribution shift (DS), where training and test data come from two different distributions: the training data are drawn from $p_s(\mathbf{x}, y)$, the test data are drawn from $p_t(\mathbf{x}, y)$, and $p_s(\mathbf{x}, y) \neq p_t(\mathbf{x}, y)$. Under DS, supervised deep learning can lead to deep classifiers biased to the training data whose performance may significantly drop on the test data. In this work, we focus on learning with noisy labels, one of the most popular DS settings where $p_s(\mathbf{x}) = p_t(\mathbf{x})$ and $p_s(y|\mathbf{x}) \neq p_t(y|\mathbf{x})$. (Ye et al., 2019; Fang et al., 2020)

As DNNs can essentially memorize any (even random) labeling of data, noisy labels have a drastic effect on the gen-

eralization performance of DNNs. Many approaches have been proposed to improve the robustness against noisy data for learning with noisy labels. Robustness to label noise can be pursued by identifying noisy samples to reduce their contribution to the loss (Han et al., 2018; Mirzasoleiman et al., 2020), correct their labels (Yi & Wu, 2019; Li et al., 2020), utilize the robust loss function (Zhang & Sabuncu, 2018; Wang et al., 2019) and regularization (Liu et al., 2020). While these existing methods are effective in mitigating label noise, since their criterion for identifying noisy examples uses the posterior information of the corrupted network, the network may suffer from undesirable bias. Recent studies point out that existing methods utilize biased information from corrupted networks. (Kim et al., 2021a)

While previous regularization-based learning frameworks (Cao et al., 2020; Xia et al., 2020) alleviate this problem, these methods require a lot of computational resources and are difficult to apply in practice. To mitigate such impractical issues for previous research, we provide a label-noise-aware learning framework with an efficient regularization method. Through the theoretical analysis that LS implicitly causes Lipschitz regularization, our proposed framework, coined as ALASCA, applies LS on sub-classifiers with varying regularization strength depending on the particular data point. The strength is larger for low confidence instances that most of the noisy instances are included. Unlike the previous regularization-based approaches, our ALASCA is a practical application of Lipschitz regularization on intermediate layer by using adaptive LS and sub-classifiers. We show that ALASCA is a universal framework by combining and comparing existing learning with noisy label (LNL) methods and validate that it consistently improves the generalization.

2. Robust Training via Label Smoothing

2.1. Label Smoothing as Lipschitz Regularization

2.1.1. THEORETICAL MOTIVATION

Lipschitz regularization (LR) has been shown to be effective for DNNs. (Terjék, 2019; Gouk et al., 2021) In this section, with the success of LR, we analytically present our motivation that LS implicitly encourages LR. Here, we formally define notation and terminology for our problem.

¹Kim Jaechul Graduate School of AI, KAIST, Seoul, South Korea ²Department of Statistics and Operations Research, University of North Carolina at Chapel Hill. Correspondence to: Se-Young Yun <yunseyoung@kaist.ac.kr>.

Table 1. Main findings regarding LS and label noise in recent works and our work.

	Main findings	Conclusion
Lukasik et al. (2020)	LS has loss correction and ℓ_2 regularization effects.	LS improves robustness.
Wei et al. (2021)	LS tends to over-smooth the estimated posterior.	LS can hurt robustness.
Our work	LS implicitly incurs Lipschitz regularization.	ALS on sub-classifier improves robustness.

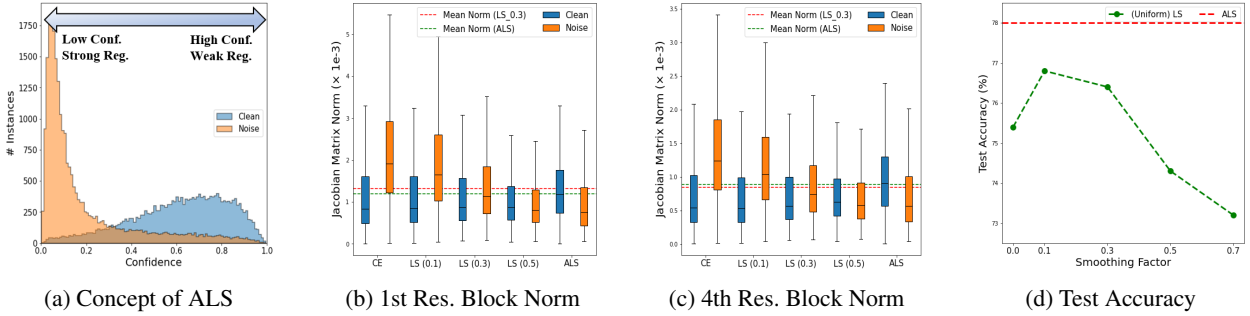


Figure 1. (a) The concept of ALS. Since noisy instances tend to have lower confidence, we conduct stronger regularization on lower confidence instances. (b)-(c) Comparison of norm of Jacobian matrix for last residual blocks. We can see that both norm of Jacobian for clean and noisy instances are reducing by increasing smoothing factor which validate our theoretical results. While mean of Jacobian norm across total instances are similar in LS (0.3) and ALS, ALS applies different power of regularization for clean and noisy instances. (d) Test accuracies for various smoothing factors of LS and ALS.

Notation. We focus on multiclass classification with L classes. Assume that the data points and labels lie in $\mathcal{X} \times \mathcal{Y}$, where the feature space $\mathcal{X} \subset \mathbb{R}^D$ and label space $\mathcal{Y} = \{0, 1\}^L$. A single data point \mathbf{x} and its label \mathbf{e}_y (i.e. one-hot vector for label y) follow a distribution $(\mathbf{x}, \mathbf{e}_y) \sim P_{\mathcal{X} \times \mathcal{Y}}$. Our goal is to find a predictor $\mathbf{f} : \mathcal{X} \rightarrow \mathbb{R}^L$ minimizing the risk of $\mathbb{E}_{(\mathbf{x}, \mathbf{e}_y) \sim P_{\mathcal{X} \times \mathcal{Y}}} [\ell(\mathbf{f}(\mathbf{x}), \mathbf{e}_y)]$ with loss function $\ell : \mathbb{R}^L \times \mathbb{R}^L \rightarrow \mathbb{R}_+$.

Compared to cross-entropy (CE) loss with one-hot vector $\ell(\mathbf{f}(\mathbf{x}), \mathbf{e}_y)$, CE loss with LS $\ell(\mathbf{f}(\mathbf{x}), \bar{\mathbf{e}}_y)$ of factor α can be presented as follows:

$$\ell(\mathbf{f}(\mathbf{x}), \bar{\mathbf{e}}_y) \propto \ell(\mathbf{f}(\mathbf{x}), \mathbf{e}_y) + \frac{\alpha}{(1-\alpha) \cdot L} \cdot \Omega(\mathbf{f}),$$

where $\mathbf{1}$ denotes all-one vector and $\bar{\mathbf{e}}_y = (1-\alpha)\mathbf{e}_y + \alpha\mathbf{1}$. With denoting $f_i(\cdot)$ as i -th element of logit value, $\mathbf{f}(\cdot)$, the regularization term of LS is

$$\Omega(\mathbf{f}) = L \cdot \log \left[\sum_{i=1}^L e^{f_i(\cdot)} \right] - \sum_{i=1}^L f_i(\cdot) \quad (1)$$

Recently, Lukasik et al. (2020) suggested the perspective that LS encourages weight shrinkage of DNN, however, this interpretation is only validated in the linear model. To understand the LS more closely, we consider that function of DNNs can be presented as arbitrary surrogate models. We suppose that the surrogate model $\mathbf{f}(\cdot) = \mathbf{g} \circ \mathbf{h}(\cdot)$ consists of $\mathbf{h} : \mathcal{X} \rightarrow \mathbb{R}^Q$ which is arbitrary twice differen-

table function for feature extractor and fixed linear classifier $\mathbf{g}(\mathbf{z}) = \mathbf{W}^\top \mathbf{z}$ with $\mathbf{W} \in \mathbb{R}^{Q \times L}$ and $\mathbf{z} \in \mathbb{R}^Q$. To establish our theorem, we assume the following reasonable conditions:

Assumption 2.1. $\mathbf{W}_1, \mathbf{W}_2, \dots, \mathbf{W}_L$ is an affine basis of \mathbb{R}^Q , where \mathbf{W}_i is the i -th column of \mathbf{W} . (i.e., $\mathbf{W}_2 - \mathbf{W}_1, \mathbf{W}_3 - \mathbf{W}_1, \dots, \mathbf{W}_L - \mathbf{W}_1$ are linearly independent.)

Assumption 2.2. Each gradient $\nabla h_i(\mathbf{x})$ is Lipschitz continuous with a Lipschitz constant L_h for all i , where $\mathbf{h}(\mathbf{x}) = (h_1(\mathbf{x}), h_2(\mathbf{x}), \dots, h_Q(\mathbf{x}))$.

Theorem 2.3. $\Omega(\mathbf{f})$ is minimized when $\mathbf{h}(\mathbf{x}) = \mathbf{0}$ for all \mathbf{x} (*) and if weight matrix \mathbf{W} satisfies Assumption 2.1, (*) is unique minimizer. Furthermore, with Assumption 2.2, $\|\mathbf{J}_{\mathbf{f}}(\mathbf{x})\|_F \rightarrow \mathbf{0}$ as $N \rightarrow \infty$ holds, where $\mathbf{J}_{\mathbf{f}}$ is the Jacobian matrix of \mathbf{f} .

Theorem 2.3 states that the LS encourages smoothness of feature extractor functions which is the same in effect as LR. The detailed proof can be found in the subsection B.1. Our perspective can explain the data-dependent regularization, while Lukasik et al. (2020) which interprets LS as regularization on the weight matrix shared by all data points cannot. This perspective of LS enables us to adaptive LR to apply different smoothing factors.

2.1.2. IMPORTANCE OF ADAPTIVE REGULARIZATION

Under label noise, we need regularization to mitigate the risk that deep classifiers are biased toward the training data, and

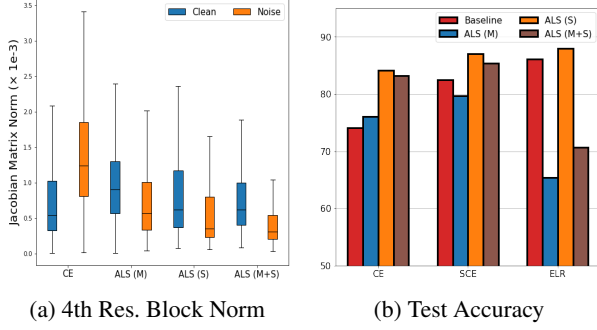


Figure 2. Comparison between ALS on main (M) and sub-classifiers (S). Conducting ALS on sub-classifiers only regularize Lipschitzness of feature extractor efficiently without any ”over-smooth” issue of main classifier.

the performance significantly drop on the test data. However, uniformly weak regularization may overfit on noisy data, whereas uniformly strong regularization causes underfitting on the clean data. Hence, we need adaptive regularization which set proper instance-dependent regularization power. Previously, many studies show that different regularization strength along the data points is essential. Wang et al. (2013) and Tibshirani (2014) state that smoothing splines with different smoothing parameters performs well. Cao et al. (2020) shows that applying stronger LR to high uncertainty data points improves generalization on noisy datasets. To implement adaptive LR through LS, we design a smoothing factor of LS for each instance as proportional to the $1 - \Pr(y|\mathbf{x})$. The loss function with ALS is as follows:

$$\ell_{ALS}(\mathbf{f}(\mathbf{x}), \mathbf{e}_y) = \beta \cdot \ell(\mathbf{f}(\mathbf{x}), \mathbf{e}_y) + (1 - \beta) \cdot \Omega(\mathbf{f}), \quad (2)$$

where β is y -th element of $\text{Softmax}(\mathbf{f}(\mathbf{x}))$. This designation of smoothing factor is motivated from theoretical results of Cao et al. (2020).

To evaluate the importance of adaptive regularization, we compute the norm of Jacobian matrix for last layer of all residual blocks of ResNet34 trained on CIFAR-10 with symmetric 60% noise. The detailed experimental settings are in Appendix. In Figure 1, we observe that the norm of both clean and noisy instances tends to decrease as the smoothing factor becomes larger. These results validate that theoretical analysis that LS incurs LR. However, by using ALS, the norm of clean instances is larger than the noisy instances, since we conduct stronger regularization for lower confidence instances, where noisy instances take up a large proportion. Furthermore, while LS with mostly smoothing factor degrades the performance, which is consistent with results in Wei et al. (2021), our ALS slightly improves generalization performance.

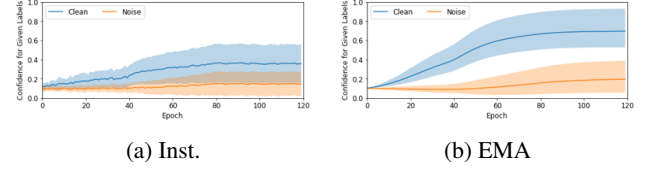


Figure 3. Dynamic patterns (mean \pm std) of (a) instantaneous confidence and (b) EMA confidence suggested in our ALASCA under CIFAR10 Sym 80% noise. Larger gap between curves is better.

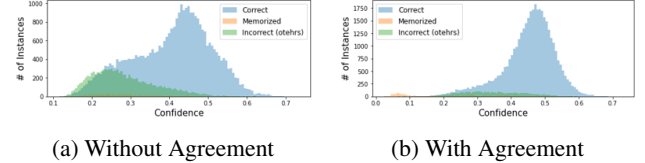


Figure 4. Confidence for selected target of main classifier (a) without and (b) with agreement with main classifier and sub-classifier at 20th epoch under Sym 60% noise.

2.2. ALASCA: Adaptive Label smoothing on Sub-Classifier for learning with noisy labels

2.2.1. MAIN MOTIVATION: IMPORTANCE OF REGULARIZING INTERMEDIATE LAYER

Recent studies have emphasized LR of intermediate layers. Wei & Ma (2019a;b) show that regularizing the Lipschitzness of all intermediate layer improves the generalization of DNNs. Sokolić et al. (2017) and Cao et al. (2020) show similar results in data-limited and distribution shift settings, respectively. However, the main weakness of this explicit regularization is that it needs multiple training phases to estimate and apply the relative regularization power for different data points.

To overcome the computation issues of the existing methods, motivated by Zhang et al. (2019) and Lee et al. (2021), we apply ALS on sub-classifiers attached to intermediate layers to enable adaptive LR of intermediate layer efficiently. By using this approach, we can encourage greater LR to noisy instances and weaker LR to clean instances with negligible additional computation. Since we agree with observations in Wei et al. (2021) from Figure 1d, we do not conduct LS on main classifier. It incurs adaptive LR as in Figure 2a, but does not affect to ”over-smooth” of the main classifier. We empirically validate that conducting ALS only on sub-classifiers has higher performance in Figure 2b.

2.2.2. PROPOSED METHOD

In this section, we present our proposed label-noise-aware learning framework, ALASCA, which applies ALS to sub-classifiers. The main consideration of adding sub-classifier is to regularize the intermediate layer for training feature extractor robustly. The training process of ALASCA includes

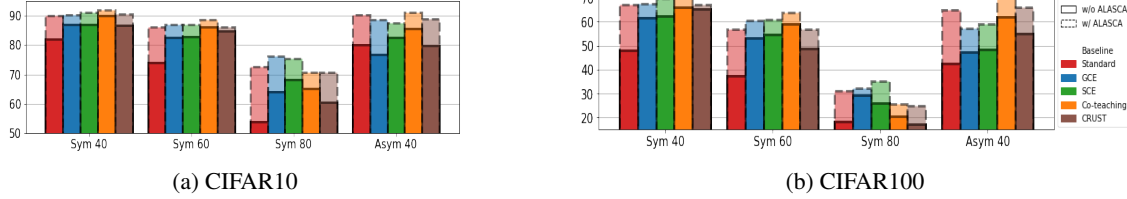


Figure 5. Comparison of performance gains by applying ALASCA to existing LNL methods under different noise types and fractions on CIFAR10 and 100. The results of all baseline methods were taken from (Liu et al., 2020; Kim et al., 2021a). The average accuracies over five trials are reported.

two components, which are introduced as follows:

1. **EMA Confidence:** As we can see in Figure 3a, instantaneous confidence suffers from high variance across training epochs and is inaccurate for clean data detection. Incorrectly determined regularization power due to such instability leads to performance degradation. We use exponential moving average (EMA) along the epochs to compute confidence for solving this issue.
2. **Label Correction with Agreement:** Compared to ALS on sub-classifiers, self-knowledge distillation (Zhang et al., 2019) have additional label correction effects. However, we observed that this correction could be led to sub-optimal since it uses posterior information of corrupted networks. To train the feature extractor more robustly, we additionally propose to correct the label only if the main classifier and sub-classifiers make the same predictions. While Figure 4a shows that main classifier highly transfer incorrect targets to sub-classifier, using agreement mitigate this issues as shown in Figure 4b.

2.2.3. FORMULATION

The loss function of ALASCA is as follows:

$$\mathcal{L} = \ell_{LNL}(\mathbf{q}^C, e_y) + \lambda \cdot \sum_{i=1}^{C-1} \ell(\mathbf{q}^i, \gamma \cdot \hat{e}_y + (1-\gamma) \cdot \mathbf{1}) \quad (3)$$

where ℓ_{LNL} is the loss function for the main classifier which can be any loss function of existing LNL methods (e.g., GCE, Co-teaching) and ℓ is the CE function for sub-classifiers. Note that \mathbf{q}^i denotes the logit vector for i -th classifier, λ is a hyperparameter for overall regularization strength. Because of the lack of space, we describe in detail about EMA confidence γ and corrected label by agreement \hat{e}_y in Appendix C.

3. Experiments

To verify the superiority of ALASCA, we combine and compare our proposed method with various existing LNL methods and identify that ours consistently improves the generalization in the presence of noise labels. The related work, experimental setups, and additional results are detailed in Appendix.

Table 2. Comparison of performances with self-knowledge distillation methods under different noise types and fractions (%) on CIFAR10.

	Sym 40	Sym 60	Sym 80	Asym 40
ONE	89.4 \pm 0.2	84.2 \pm 0.6	66.4 \pm 0.4	89.7 \pm 0.1
BYOT	89.3 \pm 0.1	84.3 \pm 0.4	70.5 \pm 0.7	88.1 \pm 0.3
ALASCA	90.9 \pm 0.1	86.2 \pm 0.2	72.7 \pm 0.6	91.2 \pm 0.1

Table 3. Comparison with state-of-the-art methods in test accuracy (%) on Clothing1M dataset. Results for baselines are copied from Kim et al. (2021a). The best results for using single network and 2 networks are highlighted in underline and bold.

Standard	GCE	SCE	DivideMix	ELR+
68.94	69.75	71.02	74.76	74.81
JoCoR	FINE	ALASCA	A-DivideMix	A-ELR+
70.30	72.91	<u>74.14</u>	75.12	75.05

3.1. Main Results

3.1.1. RESULT WITH SYNTHETIC DATASETS

Comparison with Existing LNL Methods Figure 5 provides the performance of different LNL methods on various noise distributions and datasets. In general, ALASCA achieved the highest test accuracy in several noise settings on both datasets. Furthermore, we observe that ALASCA is a universal framework that can be extended to various LNL methods and obtain a consistent test accuracy improvement.

Comparison with Existing Distillation Methods Since our ALASCA can be viewed as self-knowledge distillation framework, we compare our ALASCA with existing distillation methods. In Table 2, our ALASCA shows the best performance over the baseline self-knowledge distillation methods. (Lan et al., 2018; Zhang et al., 2019)

3.1.2. RESULT WITH REAL-WORLD DATASET

Clothing1M (Xiao et al., 2015) contains 1 million clothing images obtained from online shopping websites on 14 classes with an estimated noise level of 38.5% (Song et al., 2019). Table 3 compares the ALASCA, A-DivideMix,

and A-ELR+ to the state-of-the-art methods on the Clothing1M dataset. While A-DivideMix achieves state-of-the-art performances, ALASCA gets comparable performance although using single network and less computation cost.

4. Conclusion

This paper introduces a label-noise-aware learning framework, ALASCA, which regularizes more strongly on data points with noisy labels on intermediate layers. Based on our main finding that LS implicitly incurs LR with theoretical guarantees, we suggested to conduct ALS on sub-classifiers with negligible additional computation. Furthermore, our experimental results on benchmark-simulated and real-world datasets demonstrate the superiority of the ALASCA. We hope that our contribution will lower the risk of label noise and develop robust models.

References

- Arpit, D., Jastrzebski, S., Ballas, N., Krueger, D., Bengio, E., Kanwal, M. S., Maharaj, T., Fischer, A., Courville, A., Bengio, Y., et al. A closer look at memorization in deep networks. In *International Conference on Machine Learning*, pp. 233–242. PMLR, 2017.
- Bae, S., Kim, S., Ko, J., Lee, G., Noh, S., and Yun, S.-Y. Self-contrastive learning. *arXiv preprint arXiv:2106.15499*, 2021.
- Berthelot, D., Carlini, N., Goodfellow, I., Papernot, N., Oliver, A., and Raffel, C. Mixmatch: A holistic approach to semi-supervised learning. *arXiv preprint arXiv:1905.02249*, 2019.
- Cao, K., Chen, Y., Lu, J., Arechiga, N., Gaidon, A., and Ma, T. Heteroskedastic and imbalanced deep learning with adaptive regularization. *arXiv preprint arXiv:2006.15766*, 2020.
- Cheng, H., Zhu, Z., Li, X., Gong, Y., Sun, X., and Liu, Y. Learning with instance-dependent label noise: A sample sieve approach. *arXiv preprint arXiv:2010.02347*, 2020.
- Engleson, E. and Azizpour, H. Generalized jensen-shannon divergence loss for learning with noisy labels. *arXiv preprint arXiv:2105.04522*, 2021.
- Fang, T., Lu, N., Niu, G., and Sugiyama, M. Rethinking importance weighting for deep learning under distribution shift. *Advances in Neural Information Processing Systems*, 33:11996–12007, 2020.
- Ghosh, A., Kumar, H., and Sastry, P. Robust loss functions under label noise for deep neural networks. In *Proceedings of the AAAI Conference on Artificial Intelligence*, volume 31, 2017.
- Gouk, H., Frank, E., Pfahringer, B., and Cree, M. J. Regularisation of neural networks by enforcing lipschitz continuity. *Machine Learning*, 110(2):393–416, 2021.
- Han, B., Yao, Q., Yu, X., Niu, G., Xu, M., Hu, W., Tsang, I., and Sugiyama, M. Co-teaching: Robust training of deep neural networks with extremely noisy labels. *arXiv preprint arXiv:1804.06872*, 2018.
- Hinton, G., Vinyals, O., and Dean, J. Distilling the knowledge in a neural network. *arXiv preprint arXiv:1503.02531*, 2015.
- Kim, T., Ko, J., Cho, S., Choi, J., and Yun, S.-Y. Fine samples for learning with noisy labels, 2021a.
- Kim, T., Oh, J., Kim, N., Cho, S., and Yun, S.-Y. Comparing kullback-leibler divergence and mean squared error loss in knowledge distillation. *arXiv preprint arXiv:2105.08919*, 2021b.
- Lan, X., Zhu, X., and Gong, S. Knowledge distillation by on-the-fly native ensemble. *arXiv preprint arXiv:1806.04606*, 2018.
- Lee, H., Shin, S., and Kim, H. Abc: Auxiliary balanced classifier for class-imbalanced semi-supervised learning. *Advances in Neural Information Processing Systems*, 34, 2021.
- Lee, K.-H., He, X., Zhang, L., and Yang, L. Cleannet: Transfer learning for scalable image classifier training with label noise. In *Proceedings of the IEEE Conference on Computer Vision and Pattern Recognition*, pp. 5447–5456, 2018.
- Li, J., Socher, R., and Hoi, S. C. Dividemix: Learning with noisy labels as semi-supervised learning. *arXiv preprint arXiv:2002.07394*, 2020.
- Liu, S., Niles-Weed, J., Razavian, N., and Fernandez-Granda, C. Early-learning regularization prevents memorization of noisy labels. *arXiv preprint arXiv:2007.00151*, 2020.
- Lukasik, M., Bhojanapalli, S., Menon, A., and Kumar, S. Does label smoothing mitigate label noise? In *International Conference on Machine Learning*, pp. 6448–6458. PMLR, 2020.
- Ma, X., Huang, H., Wang, Y., Romano, S., Erfani, S., and Bailey, J. Normalized loss functions for deep learning with noisy labels. In *International Conference on Machine Learning*, pp. 6543–6553. PMLR, 2020.
- Malach, E. and Shalev-Shwartz, S. “Decoupling” when to update” from” how to update”. *arXiv preprint arXiv:1706.02613*, 2017.

- Mirzasoleiman, B., Cao, K., and Leskovec, J. Coresets for robust training of neural networks against noisy labels. *arXiv preprint arXiv:2011.07451*, 2020.
- Müller, R., Kornblith, S., and Hinton, G. When does label smoothing help? *arXiv preprint arXiv:1906.02629*, 2019.
- Sokolić, J., Giryès, R., Sapiro, G., and Rodrigues, M. R. Robust large margin deep neural networks. *IEEE Transactions on Signal Processing*, 65(16):4265–4280, 2017.
- Song, H., Kim, M., Park, D., and Lee, J.-G. How does early stopping help generalization against label noise? *arXiv preprint arXiv:1911.08059*, 2019.
- Szegedy, C., Vanhoucke, V., Ioffe, S., Shlens, J., and Wojna, Z. Rethinking the inception architecture for computer vision. In *Proceedings of the IEEE conference on computer vision and pattern recognition*, pp. 2818–2826, 2016.
- Tanaka, D., Ikami, D., Yamasaki, T., and Aizawa, K. Joint optimization framework for learning with noisy labels. In *Proceedings of the IEEE Conference on Computer Vision and Pattern Recognition*, pp. 5552–5560, 2018.
- Terjék, D. Adversarial lipschitz regularization. *arXiv preprint arXiv:1907.05681*, 2019.
- Tibshirani, R. J. Adaptive piecewise polynomial estimation via trend filtering. *The Annals of Statistics*, 42(1):285–323, 2014.
- Veit, A., Alldrin, N., Chechik, G., Krasin, I., Gupta, A., and Belongie, S. Learning from noisy large-scale datasets with minimal supervision. In *Proceedings of the IEEE conference on computer vision and pattern recognition*, pp. 839–847, 2017.
- Wang, X., Du, P., and Shen, J. Smoothing splines with varying smoothing parameter. *Biometrika*, 100(4):955–970, 2013.
- Wang, Y., Ma, X., Chen, Z., Luo, Y., Yi, J., and Bailey, J. Symmetric cross entropy for robust learning with noisy labels. In *Proceedings of the IEEE/CVF International Conference on Computer Vision*, pp. 322–330, 2019.
- Wei, C. and Ma, T. Data-dependent sample complexity of deep neural networks via lipschitz augmentation. *arXiv preprint arXiv:1905.03684*, 2019a.
- Wei, C. and Ma, T. Improved sample complexities for deep networks and robust classification via an all-layer margin. *arXiv preprint arXiv:1910.04284*, 2019b.
- Wei, J., Liu, H., Liu, T., Niu, G., and Liu, Y. Understanding generalized label smoothing when learning with noisy labels. *arXiv preprint arXiv:2106.04149*, 2021.
- Xia, X., Liu, T., Han, B., Gong, C., Wang, N., Ge, Z., and Chang, Y. Robust early-learning: Hindering the memorization of noisy labels. In *International Conference on Learning Representations*, 2020.
- Xiao, T., Xia, T., Yang, Y., Huang, C., and Wang, X. Learning from massive noisy labeled data for image classification. In *Proceedings of the IEEE conference on computer vision and pattern recognition*, pp. 2691–2699, 2015.
- Ye, Q., Liu, L., Zhang, M., and Ren, X. Looking beyond label noise: Shifted label distribution matters in distantly supervised relation extraction. *arXiv preprint arXiv:1904.09331*, 2019.
- Yi, K. and Wu, J. Probabilistic end-to-end noise correction for learning with noisy labels. In *Proceedings of the IEEE/CVF Conference on Computer Vision and Pattern Recognition*, pp. 7017–7025, 2019.
- Yu, X., Han, B., Yao, J., Niu, G., Tsang, I., and Sugiyama, M. How does disagreement help generalization against label corruption? In *International Conference on Machine Learning*, pp. 7164–7173. PMLR, 2019.
- Yuan, L., Tay, F. E., Li, G., Wang, T., and Feng, J. Revisiting knowledge distillation via label smoothing regularization. In *Proceedings of the IEEE/CVF Conference on Computer Vision and Pattern Recognition*, pp. 3903–3911, 2020.
- Zhang, C., Bengio, S., Hardt, M., Recht, B., and Vinyals, O. Understanding deep learning requires rethinking generalization, 2017a.
- Zhang, H., Cisse, M., Dauphin, Y. N., and Lopez-Paz, D. mixup: Beyond empirical risk minimization. *arXiv preprint arXiv:1710.09412*, 2017b.
- Zhang, L., Song, J., Gao, A., Chen, J., Bao, C., and Ma, K. Be your own teacher: Improve the performance of convolutional neural networks via self distillation. In *Proceedings of the IEEE/CVF International Conference on Computer Vision*, pp. 3713–3722, 2019.
- Zhang, Z. and Sabuncu, M. R. Generalized cross entropy loss for training deep neural networks with noisy labels. In *32nd Conference on Neural Information Processing Systems (NeurIPS)*, 2018.
- Zhang, Z. and Sabuncu, M. R. Self-distillation as instance-specific label smoothing. *arXiv preprint arXiv:2006.05065*, 2020.
- Zhou, X., Liu, X., Jiang, J., Gao, X., and Ji, X. Asymmetric loss functions for learning with noisy labels. *arXiv preprint arXiv:2106.03110*, 2021.

Appendix: Rethinking Label Smoothing for Deep Learning Under Label Noise

A. Related Works

A.1. Learning with Noise Label

(Zhang et al., 2017a) empirically showed that any convolutional neural networks trained using stochastic gradient methods easily fit a random labeling of the training data. To tackle this issue, numerous works have examined the classification task with noisy labels. Existing methods address this problem by (1) filtering out the noisy examples and only using clean examples for training (Malach & Shalev-Shwartz, 2017; Han et al., 2018; Mirzasoaleiman et al., 2020; Kim et al., 2021a) or (2) relabeling the noisy examples by the model itself or another model trained only on a clean dataset (Tanaka et al., 2018; Lee et al., 2018; Yi & Wu, 2019; Li et al., 2020; Liu et al., 2020). Some approaches focus on designing loss functions that have robust behaviors and provable tolerance to label noise (Ghosh et al., 2017; Zhang & Sabuncu, 2018; Wang et al., 2019; Ma et al., 2020; Zhou et al., 2021; Engleson & Azizpour, 2021).

Regularization-based Methods. Another line of works has attempted to design regularization based techniques. For example, some studies have stated that the early-stopped model can prevent the memorization phenomenon for noisy labels (Arpit et al., 2017; Song et al., 2019) and theoretically analyzed it. Based on this intuition, (Liu et al., 2020) proposed an ELR loss function to prohibit memorizing noisy data by leveraging the semi-supervised learning (SSL) techniques. (Xia et al., 2020) clarified which neural network parameters cause memorization and proposed a robust training strategy for these parameters. Efforts have been made to develop regularizations on the prediction level by smoothing the one-hot vector (Lukasik et al., 2020), using linear interpolation between data instances (Zhang et al., 2017b), and distilling the rescaled prediction of other models (Müller et al., 2019; Kim et al., 2021b). Recently, (Cao et al., 2020) proposed heteroskedastic adaptive regularization which applies stronger regularization to noisy instances.

Noise-Cleansing based Approaches. Existing methods address this problem by (1) filtering out the noisy data and only using the clean data for training or (2) relabeling the noisy data by the model during training or by another model trained only on a clean dataset. Firstly, for sample selection approaches, (Malach & Shalev-Shwartz, 2017) suggested decoupling method that trains two networks simultaneously, and then updates models only using the instances that have different predictions from two networks. (Han et al., 2018) proposed a noisy detection approaches, named co-teaching, that utilizes two networks, extracts subsets of instances with small losses from each network, and trains each network with subsets of instances filtered by another network. Recently, new noisy detector with theoretical support have been developed. (Mirzasoaleiman et al., 2020) introduced an algorithm that selects subsets of clean instances that provide an approximately low-rank Jacobian matrix and proved that gradient decent applied to the subsets prevent overfitting to noisy labels. (Kim et al., 2021a) proposed detecting framework, termed FINE which utilize the high-order topological information of data in latent space by using eigen decomposition of their covariance matrix. Secondly, for label correction approaches, (Veit et al., 2017) provided a semi-supervised learning framework that facilitates small sets of clean instances and an additional label cleaning network to correct the massive sets of noisy labels. (Tanaka et al., 2018) proposed a joint optimization framework that optimizes the network parameters and class labels using an alternative strategy. (Lee et al., 2018) introduced CleanNet, which learns a class-embedding vector and a query-embedding vector with a similarity matching constraint to identify the noise instances that have less similar embedding vectors with their class-embedding vectors. (Yi & Wu, 2019) provided a probabilistic learning framework that utilizes label distribution updated by back-propagation to correct the noisy labels. Recently, (Li et al., 2020) modeled the per-sample loss distribution and divide it into a labeled set with clean samples and an unlabeled set with noisy samples, and they leverage the noisy samples through the well-known semi-supervised learning technique MixMatch (Berthelot et al., 2019).

Robust Loss Functions. Some approaches focus on designing loss functions that have robust behaviors and provable tolerance to label noise. (Ghosh et al., 2017) theoretically proved that the mean absolute error (MAE) might be robust against noisy labels while commonly used cross-entropy loss are not. (Zhang & Sabuncu, 2018) argued that MAE performed poorly with DNNs and proposed a GCE loss function, which can be seen as a generalization of MAE and CE. (Wang et al., 2019) introduced the reverse version of the cross-entropy term (RCE) and suggested the SCE loss function as a weighted sum of CE and RCE. (Ma et al., 2020) showed that normalized version of any loss would be robust to noisy labels. Recently, (Zhou et al., 2021) argued that symmetric condition of existing robust loss function is overly restrictive and proposed asymmetric

loss function families which alleviate symmetric condition while maintain noise-tolerant of noise robust loss function.

A.2. Label Smoothing

Smoothing the label \mathbf{y} is a common method for improving the performance of DNNs by preventing the over-confident predictions (Szegedy et al., 2016). LSR is a technique that facilitates the generalization by replacing a ground-truth one-hot vector \mathbf{y} with a weighted mixture of hard targets $\bar{\mathbf{y}}$:

$$\bar{y}_k = \begin{cases} (1 - \alpha) + \frac{\alpha}{L} & \text{if } y_k = 1 \\ \frac{\alpha}{L} & \text{otherwise,} \end{cases}$$

where k denotes the index, L denotes number of classes, and α is a constant. (Lukasik et al., 2020) argued that LS denoise label noise by causing label correction effect and weight shrinkage regularization effect. (Yuan et al., 2020) demonstrated that KD might be a category of LS by using the adaptive noise (i.e., KD is a label regularization method). Recently, Wei et al. (2021) theoretically show that the LS incurs over-smooth of classifiers and leads to performance degradation under severe noise rates.

Knowledge Distillation. Several works have attempted to view knowledge distillation (KD) as learned LS. The goal of KD (Hinton et al., 2015) is to effectively train a simpler network called student network by transferring the knowledge of a pretrained complex network. Although KD used in a wide of range, however, there are two distinct limitations: 1) KD requires pre-training of the complex teacher model, and 2) variation of the teacher networks will result in different performances with same student network. To mitigate these issues, self-distillation approaches have been proposed to enhances the effectiveness of training a student network by utilizing its own knowledge without a teacher network. (Zhang et al., 2019) introduced self-distillation method which utilize auxiliary weak classifier networks that classify the output with the feature from the middle-hidden layers. Recently, (Zhang & Sabuncu, 2020) view self-distillation as instance-specific LS.

B. Theoretical Motivation for ALASCA Framework

B.1. Proof of Theorem 1

Definition B.1. (Lipschitzness) A continuously differentiable function \mathbf{f} is called Lipschitz continuous with a Lipschitz constant $L_f \in [0, \infty)$ if

$$\|\mathbf{f}(\mathbf{x}_i) - \mathbf{f}(\mathbf{x}_j)\| \leq L_f \|\mathbf{x}_i - \mathbf{x}_j\| \quad (4)$$

for all $\mathbf{x}_i, \mathbf{x}_j \in \text{dom } \mathbf{f}$

Definition B.2. (Lipschitz Regularization) For $\mathcal{F} : \mathbb{R}^D \rightarrow \mathbb{R}^L$ be a twice-differentiable model family. The definition of Lipschitz regularization is aiming to optimize the function with smoothness penalty as follows:

$$\min_{\mathbf{f} \in \mathcal{F}} \frac{1}{N} \sum_{n=1}^N \ell(\mathbf{f}(\mathbf{x}_n), \mathbf{y}_n) + \lambda \|\mathbf{J}_{\mathbf{f}}(\mathbf{x}_n)\|_F, \quad (5)$$

where λ is the regularization coefficient, N is the number of training data points, and $\mathbf{J}_{\mathbf{f}}$ is the Jacobian matrix of \mathbf{f} .

Lemma B.3. Define a function $\Phi := \Omega \circ \mathbf{g}$, i.e. $\Phi(\mathbf{z}) = \Omega(\mathbf{g}(\mathbf{z})) = \Omega(\mathbf{f})$. Then, $\Phi(\mathbf{z})$ is twice differentiable and also convex.

Proof. Let Q denote the dimension of \mathbf{z} , i.e. $\mathbf{z} \in \mathbb{R}^Q$. That is, Φ is a function from \mathbb{R}^Q to \mathbb{R} . The gradient and Hessian of $\Phi(\mathbf{z})$ is as follows:

$$\begin{aligned} \nabla \Phi(\mathbf{z}) &= \frac{\partial \Phi(\mathbf{z})}{\partial \mathbf{z}} = \frac{\partial}{\partial \mathbf{z}} \left[L \cdot \log \left[\sum_{i=1}^L e^{\langle \mathbf{W}_i, \mathbf{z} \rangle} \right] - \sum_{i=1}^L \langle \mathbf{W}_i, \mathbf{z} \rangle \right] \\ &= L \cdot \frac{\sum_{i=1}^L e^{\langle \mathbf{W}_i, \mathbf{z} \rangle} \mathbf{W}_i}{\sum_{i=1}^L e^{\langle \mathbf{W}_i, \mathbf{z} \rangle}} - \sum_{i=1}^L \mathbf{W}_i, \end{aligned} \quad (6)$$

$$\nabla^2 \Phi(\mathbf{z}) = L \cdot \frac{\sum_{i=1}^L e^{\langle \mathbf{W}_i, \mathbf{z} \rangle} \mathbf{W}_i \mathbf{W}_i^\top \cdot \sum_{i=1}^L e^{\langle \mathbf{W}_i, \mathbf{z} \rangle} - \left(\sum_{i=1}^L e^{\langle \mathbf{W}_i, \mathbf{z} \rangle} \mathbf{W}_i \right) \left(\sum_{i=1}^L e^{\langle \mathbf{W}_i, \mathbf{z} \rangle} \mathbf{W}_i^\top \right)}{\left(\sum_{i=1}^L e^{\langle \mathbf{W}_i, \mathbf{z} \rangle} \right)^2}. \quad (7)$$

Now, let's show that $\nabla^2 \Phi(\mathbf{z})$ is positive semi-definite for all $\mathbf{z} \in \mathbb{R}^Q$. For any $\mathbf{v} \in \mathbb{R}^Q$,

$$\begin{aligned} &\mathbf{v}^\top \left(\sum_{i=1}^L e^{\langle \mathbf{W}_i, \mathbf{z} \rangle} \mathbf{W}_i \mathbf{W}_i^\top \cdot \sum_{i=1}^L e^{\langle \mathbf{W}_i, \mathbf{z} \rangle} - \left(\sum_{i=1}^L e^{\langle \mathbf{W}_i, \mathbf{z} \rangle} \mathbf{W}_i \right) \left(\sum_{i=1}^L e^{\langle \mathbf{W}_i, \mathbf{z} \rangle} \mathbf{W}_i^\top \right) \right) \mathbf{v} \\ &= \sum_{i=1}^L e^{\langle \mathbf{W}_i, \mathbf{z} \rangle} (\mathbf{W}_i^\top \mathbf{v})^2 \cdot \sum_{i=1}^L e^{\langle \mathbf{W}_i, \mathbf{z} \rangle} - \left(\sum_{i=1}^L e^{\langle \mathbf{W}_i, \mathbf{z} \rangle} \mathbf{W}_i^\top \mathbf{v} \right)^2 \geq 0 \end{aligned} \quad (8)$$

by Cauchy-Schwarz Inequality. Thus, $\mathbf{v}^\top \nabla^2 \Phi(\mathbf{z}) \mathbf{v} \geq 0$ for all $\mathbf{v} \in \mathbb{R}^Q$ and this proves that $\nabla^2 \Phi(\mathbf{z})$ is positive semi-definite for all $\mathbf{z} \in \mathbb{R}^Q$ and $\Phi(\mathbf{z})$ is convex. \square

Assumption 1. $\mathbf{W}_1, \mathbf{W}_2, \dots, \mathbf{W}_L$ is an affine basis of \mathbb{R}^Q , where \mathbf{W}_i is the i -th column of \mathbf{W} . (i.e., $\mathbf{W}_2 - \mathbf{W}_1, \mathbf{W}_3 - \mathbf{W}_1, \dots, \mathbf{W}_L - \mathbf{W}_1$ are linearly independent.)

Assumption 2. Each gradient $\nabla h_i(\mathbf{x})$ is Lipschitz continuous with a Lipschitz constant L_h for all i , where $\mathbf{h}(\mathbf{x}) = (h_1(\mathbf{x}), h_2(\mathbf{x}), \dots, h_Q(\mathbf{x}))$.

Note that $\mathbf{W}_2 - \mathbf{W}_1, \mathbf{W}_3 - \mathbf{W}_1, \dots, \mathbf{W}_L - \mathbf{W}_1$ being linearly independent is equivalent to $\mathbf{W}_2 - \mathbf{W}_1, \mathbf{W}_3 - \mathbf{W}_2, \dots, \mathbf{W}_L - \mathbf{W}_{L-1}$ being linearly independent in Assumption 2.1. Both of these will be used in the proof of

Theorem 2.3.

Theorem 1. $\Omega(\mathbf{f})$ is minimized when $\mathbf{h}(\mathbf{x}) = \mathbf{0}$ for all \mathbf{x}^* and if weight matrix \mathbf{W} satisfies Assumption 2.1, $(*)$ is unique minimizer. Furthermore, with Assumption 2.2, $\|\mathbf{J}_{\mathbf{f}}(\mathbf{x})\|_F \rightarrow \mathbf{0}$ as $N \rightarrow \infty$ holds, where $\mathbf{J}_{\mathbf{f}}$ is the Jacobian matrix of \mathbf{f} .

Proof. We specify the domain and codomain of each function: $\mathbf{g} : \mathbb{R}^Q \rightarrow \mathbb{R}^L$, $\mathbf{h} : \mathcal{X} \rightarrow \mathbb{R}^Q$ where $\mathcal{X} \subset \mathbb{R}^D$. Then,

$$\left. \frac{\partial \Omega(\mathbf{f})}{\partial \mathbf{z}} \right|_{\mathbf{z}=\mathbf{0}} = L \cdot \frac{\sum_{i=1}^L e^{\langle \mathbf{W}_i, \mathbf{z} \rangle} \mathbf{W}_i}{\sum_{i=1}^L e^{\langle \mathbf{W}_i, \mathbf{z} \rangle}} - \sum_{i=1}^L \mathbf{W}_i \Big|_{\mathbf{z}=\mathbf{0}} = \mathbf{0}. \quad (9)$$

Since $\Omega(\mathbf{f})$ is convex respect to \mathbf{z} by Lemma B.3, $\mathbf{z} = \mathbf{h}(\mathbf{x}) = \mathbf{0}$ is the global minimizer of $\Omega(\mathbf{f})$. Now, by Assumption 2.1, $\mathbf{W}_2 - \mathbf{W}_1, \mathbf{W}_3 - \mathbf{W}_1, \dots, \mathbf{W}_L - \mathbf{W}_1$ are linearly independent and is a basis for \mathbb{R}^Q . We express $\frac{\partial \Omega(\mathbf{f})}{\partial \mathbf{z}}$ with the basis as follows:

$$\begin{aligned} \frac{\partial \Omega(\mathbf{f})}{\partial \mathbf{z}} &= L \cdot \frac{\sum_{i=1}^L e^{\langle \mathbf{W}_i, \mathbf{z} \rangle} \mathbf{W}_i}{\sum_{i=1}^L e^{\langle \mathbf{W}_i, \mathbf{z} \rangle}} - \sum_{i=1}^L \mathbf{W}_i \\ &= L \cdot \frac{\sum_{i=1}^L e^{\langle \mathbf{W}_i - \mathbf{W}_1, \mathbf{z} \rangle} \mathbf{W}_i}{\sum_{i=1}^L e^{\langle \mathbf{W}_i - \mathbf{W}_1, \mathbf{z} \rangle}} - \sum_{i=1}^L \mathbf{W}_i \\ &= L \cdot \frac{\sum_{i=1}^L e^{\langle \mathbf{W}_i - \mathbf{W}_1, \mathbf{z} \rangle} (\mathbf{W}_i - \mathbf{W}_1)}{\sum_{i=1}^L e^{\langle \mathbf{W}_i - \mathbf{W}_1, \mathbf{z} \rangle}} - \sum_{i=1}^L (\mathbf{W}_i - \mathbf{W}_1). \end{aligned} \quad (10)$$

Since $\{\mathbf{W}_j - \mathbf{W}_1 : 2 \leq j \leq L\}$ forms a basis, we have

$$\begin{aligned} \frac{\partial \Omega(\mathbf{f})}{\partial \mathbf{z}} = \mathbf{0} &\iff L \cdot \frac{e^{\langle \mathbf{W}_j - \mathbf{W}_1, \mathbf{z} \rangle}}{\sum_{i=1}^L e^{\langle \mathbf{W}_i - \mathbf{W}_1, \mathbf{z} \rangle}} - 1 = 0 \quad \text{for all } 1 \leq j \leq L \\ &\iff \langle \mathbf{W}_j - \mathbf{W}_1, \mathbf{z} \rangle = 0 \quad \text{for all } 2 \leq j \leq L \\ &\iff \langle \mathbf{W}_i, \mathbf{z} \rangle = \langle \mathbf{W}_j, \mathbf{z} \rangle \quad \text{for all } 1 \leq i, j \leq L. \end{aligned} \quad (11)$$

We can find the optimal value \mathbf{z} which minimize $\Omega(\mathbf{f})$ by solving the $\frac{\partial \Omega(\mathbf{f})}{\partial \mathbf{z}} = \mathbf{0}$. Using Equation 11, we have $\langle \mathbf{W}_1 - \mathbf{W}_2, \mathbf{z} \rangle = \langle \mathbf{W}_2 - \mathbf{W}_3, \mathbf{z} \rangle = \dots = \langle \mathbf{W}_{L-1} - \mathbf{W}_L, \mathbf{z} \rangle = 0$ and

$$\begin{pmatrix} \mathbf{W}_1 - \mathbf{W}_2 \\ \mathbf{W}_2 - \mathbf{W}_3 \\ \vdots \\ \mathbf{W}_{L-1} - \mathbf{W}_L \end{pmatrix}^\top \mathbf{z} = \mathbf{0}. \quad (12)$$

Again by Assumption 2.1, the left multiplied matrix is a full rank square matrix. Hence, we obtain $\frac{\partial \Omega(\mathbf{f})}{\partial \mathbf{z}} = \mathbf{0} \iff \mathbf{z} = \mathbf{0}$, which implies that $\mathbf{z} = \mathbf{h}(\mathbf{x}) = \mathbf{0}$ is the unique minimizer of $\Omega(\mathbf{f})$.

Lastly, we show that when $\mathbf{h}(\mathbf{x}) = \mathbf{0}$ for all \mathbf{x} and with Assumption 2.2, $\|\mathbf{J}_{\mathbf{f}}(\mathbf{x})\|_F \rightarrow \mathbf{0}$ holds as the number of training sample N goes to ∞ . Let $\mathbf{x}_1, \mathbf{x}_2, \dots, \mathbf{x}_N$ be the data points used in our training. For all i and j , because we have $\mathbf{h}(\mathbf{x}_i) = \mathbf{h}(\mathbf{x}_{i+1}) = \mathbf{0}$, $\exists \mathbf{c}_{i,j} \in \overline{\mathbf{x}_i \mathbf{x}_{i+1}}$ s.t. $\nabla h_j(\mathbf{c}_{i,j}) = \mathbf{0}$ by the Mean Value Theorem. Then, using Assumption 2.2, we obtain

$$\|\nabla h_j(\mathbf{x}_i)\| \leq L_h \|\mathbf{x}_i - \mathbf{c}_{i,j}\| \leq L_h \|\mathbf{x}_i - \mathbf{x}_{i+1}\|. \quad (13)$$

Therefore,

$$\|\mathbf{J}_{\mathbf{h}}(\mathbf{x}_i)\|_F = \sqrt{\sum_{j=1}^Q \|\nabla h_j(\mathbf{x}_i)\|^2} \leq L_h \sqrt{Q} \|\mathbf{x}_i - \mathbf{x}_{i+1}\| \quad (14)$$

and for sufficiently large N and any $\epsilon > 0$, we can have the training set satisfy $\|\mathbf{x}_i - \mathbf{x}_{i+1}\| \leq \frac{\epsilon}{L_h \sqrt{Q}}$. This leads to

$$\|\mathbf{J}_{\mathbf{h}}(\mathbf{x}_i)\|_F \leq \epsilon \quad (15)$$

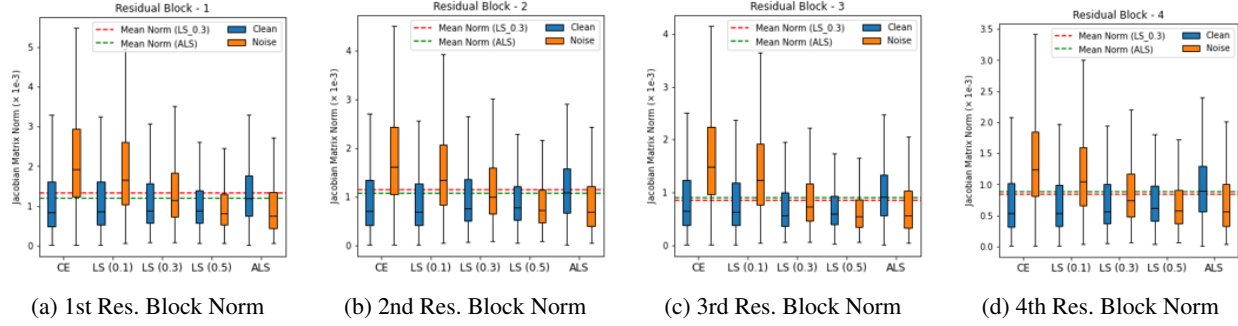


Figure 6. Overall Results for Figure 1.

which implies that $\|\mathbf{J}_h(\mathbf{x})\|_F \rightarrow 0$ as N goes to ∞ . Finally, since \mathbf{f} is a composite function of \mathbf{g} and \mathbf{h} , $\|\mathbf{J}_f(\mathbf{x})\|_F \rightarrow 0$ as $N \rightarrow \infty$ also holds. Hence, we have that the label smoothing regularizer encourages Lipschitz regularization of deep neural network functions. \square

B.2. Additional Theorem

We consider a binary classification task where $\mathcal{Y} = \{-1, 1\}$. We decompose MSE loss with LSR into MSE loss with one-hot and regularization term, and consequently show that the regularization term encourages Lipschitz regularization.

Theorem B.4. Assume that $f : [0, 1]^D \rightarrow \mathbb{R}$ is differentiable and the range includes $[-1, 1]$. Let loss function $\ell : \mathbb{R} \times \mathbb{R} \rightarrow \mathbb{R}_+$ be a square loss, i.e. $\ell(f(\mathbf{x}), y) = (f(\mathbf{x}) - y)^2$. Then, minimizing the square loss with LSR $\ell(f(\mathbf{x}), \bar{y})$ encourages Lipschitz regularization.

Proof. We can express the label smoothing term as $\bar{y} = (1 - \alpha)y$ in a binary classification problem with label -1 and 1. We decompose MSE loss with LSR as follows:

$$\begin{aligned}
 \ell(f(\mathbf{x}), \bar{y}) &= (f(\mathbf{x}) - \bar{y})^2 = (f(\mathbf{x}) - (1 - \alpha)y)^2 \\
 &= ((1 - \alpha)(f(\mathbf{x}) - y) + \alpha f(\mathbf{x}))^2 \\
 &= (1 - \alpha)^2 \ell(f(\mathbf{x}), y) + \alpha(2 - \alpha) f(\mathbf{x})^2 - 2\alpha(1 - \alpha) y f(\mathbf{x}) \\
 &= (1 - \alpha)^2 \ell(f(\mathbf{x}), y) + \alpha(2 - \alpha) \left(f(\mathbf{x}) - \frac{\bar{y}}{2 - \alpha} \right)^2 + c.
 \end{aligned} \tag{16}$$

Since f is continuous and the range includes $[-1, 1]$, there exists \mathbf{x}_0 such that $f(\mathbf{x}_0) = \frac{\bar{y}}{2 - \alpha}$. Then, by Mean Value Theorem and Cauchy-Schwarz Inequality, we obtain an upper bound of MSE loss with LSR:

$$\begin{aligned}
 \ell(f(\mathbf{x}), \bar{y}) &= (1 - \alpha)^2 \ell(f(\mathbf{x}), y) + \alpha(2 - \alpha) (f(\mathbf{x}) - f(\mathbf{x}_0))^2 + c \\
 &\approx (1 - \alpha)^2 \ell(f(\mathbf{x}), y) + \alpha(2 - \alpha) (\nabla f(\mathbf{x}) \cdot (\mathbf{x} - \mathbf{x}_0))^2 + c \\
 &\leq \ell(f(\mathbf{x}), y) + \alpha(2 - \alpha) \|\nabla f(\mathbf{x})\|^2 \|\mathbf{x} - \mathbf{x}_0\|^2 + c \\
 &\leq \ell(f(\mathbf{x}), y) + \alpha(2 - \alpha) \|\nabla f(\mathbf{x})\|^2 D + c.
 \end{aligned} \tag{17}$$

Since $\alpha(2 - \alpha)$ is an increasing function of α when $0 \leq \alpha \leq 1$, we can say that Lipschitz regularization term is included in the upper bound of $\ell(f(\mathbf{x}), \bar{y})$. Thus, we conclude that minimizing the square loss with LSR encourages Lipschitz regularization. \square

B.3. Validation of the Norm of Jacobian

According to Wei & Ma (2019a); Cao et al. (2020), existing studies replace Lipschitz regularization in intermediate layer of r -layer DNN by regularizing $R(\mathbf{x}) = \left(\sum_{j=1}^r \|\mathbf{J}^{(j)}(\mathbf{x})\|_F^2 \right)^{1/2}$ with j -th hidden layer of network $h^{(j)}$, where $\mathbf{J}^{(j)}(\mathbf{x}) := \frac{\partial}{\partial h^{(j)}} \ell(\mathbf{f}(\mathbf{x}), \mathbf{y})$ is Jacobian of the loss with respect to $h^{(j)}$. To validate our perspective, we compare the norm of Jacobian matrix for last layer of all residual blocks of ResNet34 trained on CIFAR-10 with symmetric 60% noise across different LS methods. For ALS, we used warm-up epochs as 20, for gaining an accurate regularization power coefficient β

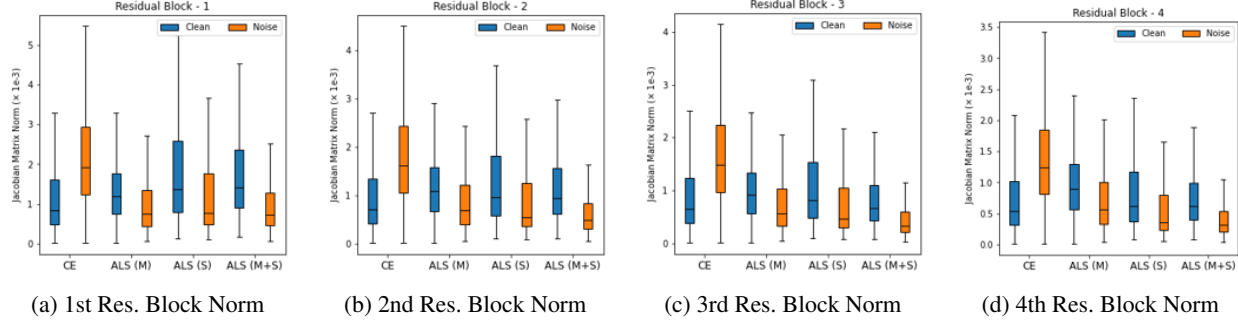


Figure 7. Overall Results for Figure 2.

during total training of 120 epochs. We can observe that ALS conduct stronger regularization on noisy instances and weaker regularization on clean instances in Figure 6. Additionally, in Figure 7, conducting ALS on sub-classifier also regularize the smoothness in instance-dependent manner.

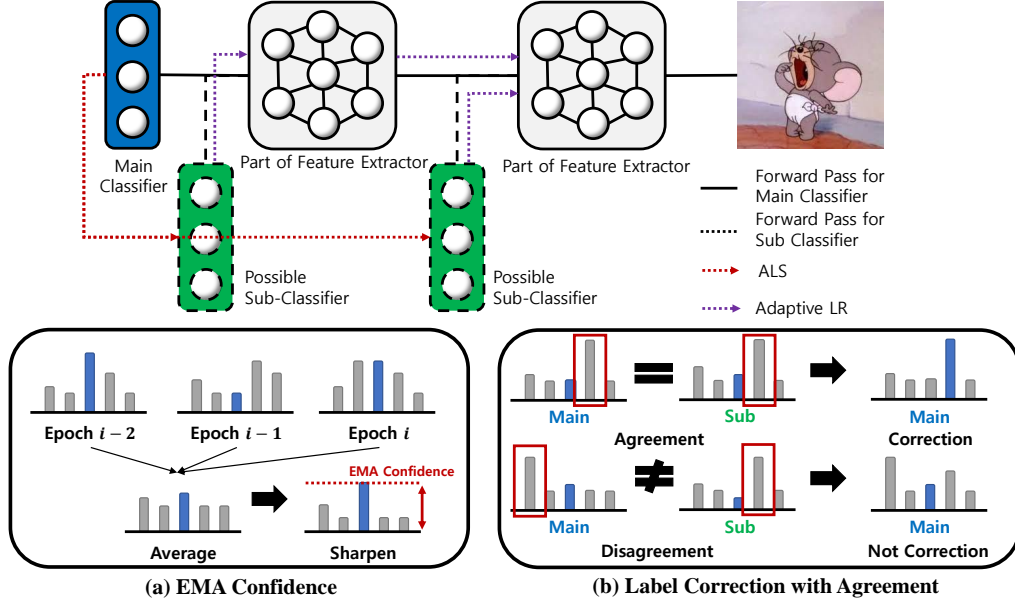


Figure 8. Overall procedure of ALASCA. (a) Since the confidence of instances at each epoch have a high variance, we compute EMA confidence for gaining stable and accurate confidence for conducting ALS. (b) Since the predictions of the main classifier would be wrong because it is posterior to a corrupted network, we modify the label of an instance when the multiple classifiers are having the same prediction which is different from the given label.

C. Supplementary Descriptions for ALASCA Algorithm

C.1. Overall Description

Motivated by (Zhang et al., 2019; Lee et al., 2021; Bae et al., 2021), We apply sub-classifier for regularizing feature extractor, while do not affect to main classifiers. As can be seen in Figure 8, the sub-classifiers can be located everywhere of networks. In our experiments, we observe that LS leads to over-smooth of main classifier and can hurt the generalization of networks under high noise rates that previously argued in (Wei et al., 2021). Although ALS in ALASCA is similar to $\text{Tf-KD}_{\text{reg}}$ in (Yuan et al., 2020), our motivation is different from $\text{Tf-KD}_{\text{reg}}$. Additionally, our most important contribution is conducting ALS on sub-classifiers to incur LR but not over-smoothing.

The loss function of ALASCA is as follows:

$$\mathcal{L} = \ell_{LNL}(\mathbf{q}^C, \mathbf{y}) + \lambda \cdot \sum_{i=1}^{C-1} \ell(\mathbf{q}^i, \gamma \cdot \hat{\mathbf{y}} + (1 - \gamma) \cdot \mathbf{1}), \quad (18)$$

where ℓ_{LNL} is the loss function for the main classifier which can be any loss function of existing LNL methods (e.g., GCE, Co-teaching) and ℓ is the cross entropy loss function for sub-classifiers. Note that \mathbf{q}^i denotes the softmax vector for i -th classifier, and α is EMA confidence and $\hat{\mathbf{y}}$ is corrected label. We set the hyperparameter for overall regularization strength λ as 2.0 for all experiments.

C.2. EMA Confidence

As seen in Figure 3 and Figure 9, the instantaneous confidence of each example have high variance across the training epoch. This enables to conduct of wrong smoothing factor for ALS which leads the feature extractor to sub-optimal. To conduct correct smoothing factor for each instance in training procedure, we apply exponential moving average for computing ALS confidence. The computation procedure for EMA confidence is as follows:

- Average : We conduct exponential moving average procedure on logit values. With EMA logit z_{EMA} , instantaneous

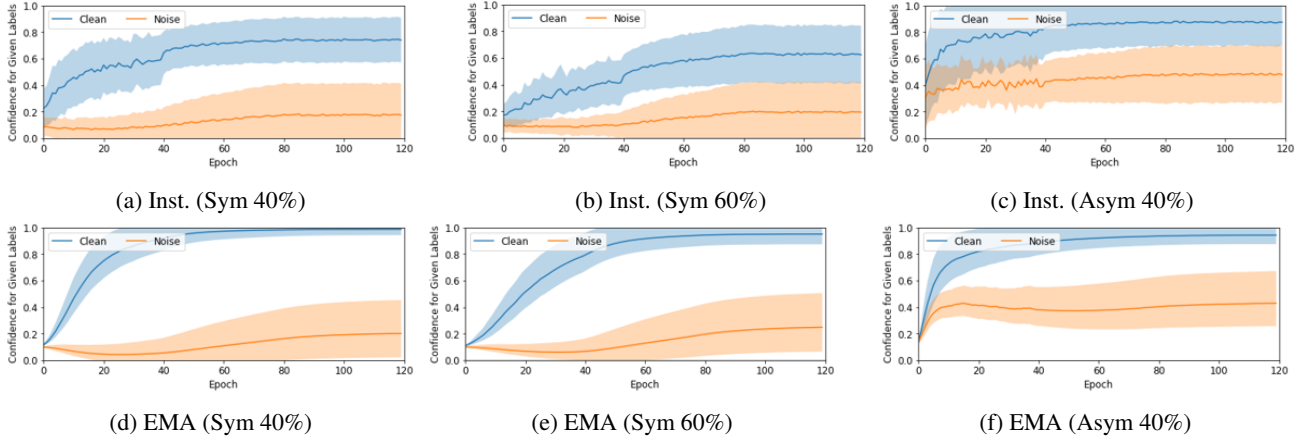


Figure 9. Dynamic patterns (mean \pm std) of (a) instantaneous confidence and (b) EMA confidence suggested in our ALASCA for CIFAR10 under various noise types and fractions. Larger gap between curves is better.

logit at t -th epoch z_t , the formula for average procedure is as follows:

$$z_{\text{EMA}} = w_{\text{EMA}} \cdot z_{\text{EMA}} + (1 - w_{\text{EMA}}) \cdot z_t$$

In our experiments, we set the initial values for EMA values as all zero vectors and the EMA weight w_{EMA} as 0.7.

- **Sharpen** : Since the averaged logits are over-smooth, which can incur weak regularization for noisy instances, and strong regularization for clean instances. Hence, we conduct sharpening the EMA logits by dividing sharpen temperature τ to logits. The final smoothing factor is as follows:

$$\gamma = \hat{y}^T \cdot \text{Softmax}(z_{\text{EMA}} \cdot \tau),$$

where \hat{y} is corrected label following by subsection C.3. We set the optimal sharpen parameter value as 3.0. By applying sharpening, we can apply very different smoothing factors to clean and noisy instances as shown in Figure 3 and Figure 9.

C.3. Label Correction with Agreement

One approach to train robust feature extractor is explicitly label correction method. Compared to LS approaches, self-knowledge distillation methods (Lan et al., 2018; Zhang et al., 2019) implicitly correction the corrupted labels, since it transfer the predictions of main classifier to sub-classifiers. While this procedure is simple yet effective, these predictions could be inaccurate since these are posterior information of corrupted networks from noisy labels.

To mitigate this problem, we provide LCA (Label Correction with Agreement), that lower the transferring inaccurate information. Overall procedure for LCA is as follows:

- Case 1: $\hat{y} = \arg \max_{i \in L} q_i^C$. If $\arg \max_{i \in L} q_i^C = \arg \max_{i \in L} q_i^{C-1}$ and $\tilde{y} \neq \arg \max_{i \in L} q_i^C$. (After warm-up epoch)
- Case 2: $\hat{y} = \tilde{y}$. Otherwise.

We observe that LCA lowers the risk that the feature extractors are corrupted by spurious information from main classifiers in Figure 4. Since the classifiers are under-fitted to train datasets for early phase, we set warm-up epoch for label correction as 20 epochs.

C.4. Sub-Classifier

As following (Zhang et al., 2019), we define the sub-classifier as a combination of a bottleneck layer and a fully connected layer. Our sub-classifiers can be positioned every part of feature extractor. To conduct a fair comparison with other self-knowledge distillation methods, we attached the sub-classifiers to the end of all residual blocks.

D. Supplementary Descriptions for Main Results

D.1. Experimental Configurations

D.1.1. NOISY LABEL GENERATION

We inject uniform randomness into a fraction of labels for symmetric noise, and flip a label only to a specific class for asymmetric noise. For example, we generate asymmetric noise by mapping TRUCK \rightarrow AUTOMOBILE, BIRD \rightarrow AIRPLANE, DEER \rightarrow HORSE, CAT \rightarrow DOG for CIFAR-10. For CIFAR-100, we divide entire dataset into 20 five-size super-classes and generate asymmetric noise by changing each class to the next class within super-classes. Also, based on (Cheng et al., 2020), we generate instance-based noise and compare the performance with existing LNL methods.

For generating instance-dependent noise we follow the state-of-the-art method (Cheng et al., 2020). Define the noise rate (the global flipping rate) as ϵ . First, in order to control ϵ but without constraining all of the instances to have a same flip rate, we sample their flip rates from a truncated normal distribution $\mathcal{N}(\epsilon, 0.1^2, [0, 1])$, where $[0, 1]$ indicates the range of the truncated normal distribution. Second, we sample parameters W from the standard normal distribution for generating instance-dependent label noise. The size of W is $S \times K$, where S denotes the length of each feature.

D.1.2. HYPERPARAMETER SETUPS FOR MAIN RESULTS

Noise Robust Loss Functions. We conduct experiments with CE, GCE, SCE, ELR as mentioned in main text. We follow all experiments settings presented in the (Liu et al., 2020). We use ResNet34 models and trained them using a standard Pytorch SGD optimizer with a momentum of 0.9. We set a batch size of 128 for all experiments. We utilize weight decay of 5×10^{-4} and set the initial learning rate as 0.02, and reduce it by a factor of 100 after 40 and 80 epochs for CIFAR datasets (total 120 epochs). For noise-robust loss functions, we train the network with 0.1 as initial α value and 0.7 as final α value and linearly increasing for the first half of training epochs.

Sample-Selection Methods. In this experiment, we use ResNet34 models (or as backbone with ALASCA) and trained them using a standard Pytorch SGD optimizer with initial learning rate of 0.02 and a momentum of 0.9. We set a batch size of 128 for all experiments and utilize weight decay of 5×10^{-4} . Unlike the noise robust loss functions, we trained all baseline with our settings and reported the results. Additionally, while we use ALASCA, we use 0.1 as initial α value and 0.7 as final α value and linearly increasing for the first half of training epochs. For Decoupling and Co-teaching, we utilize the warm-up epochs as 30, and we utilize the coreset size of CRUST as 0.5.

Semi-Supervised Approaches As an extension on the experiments in original papers (Li et al., 2020; Liu et al., 2020), we conduct experiments on various noise settings. Our experiments settings follow (Li et al., 2020). We use the same hyperparameter settings written in each paper. Similar to above, while we use ALASCA, we use 0.1 as initial α value and 0.9 as final α value and linearly increasing for the first half of training epochs.

D.2. Detailed Results

Intuitively, when the representation from the feature extractor is sufficient, the classifier’s decision boundary can be robust in spite of strong noise. To verify superiority of our framework, we combine the ALASCA with various existing LNL methods and identify that ours consistently improves the generalization in the presence of noisy data: noise-robust loss functions, sample selection approaches, and semi-supervised learning (SSL) approaches.

Noise Robust Loss Functions The noise-robust loss function is to achieve a small risk for unseen clean data even when noisy labels exist in the training data. Here, we state the conjunction effects of ALASCA with various noise-robust loss functions: generalized cross entropy (GCE) (Zhang & Sabuncu, 2018), symmetric cross entropy (SCE) (Wang et al., 2019), and early-learning regularization¹ (ELR) (Liu et al., 2020). Table 4 shows that ALASCA enhances generalization in the application of noise-robust loss functions on severe noise rate settings.

¹Since ELR is similar to other robust-loss functions in that the additive term regularizes the output of the network, we classified ELR as a robust-loss function and did not compare it in Section 4.1. Instead, we orthogonally utilize ELR and ALASCA together in this section and get better performance than the original results in (Liu et al., 2020) for all experiment settings.

Table 4. Test accuracies (%) on CIFAR-10 and CIFAR-100 under different noisy types and fractions for noise-robust loss approaches. The results of all baseline methods were taken from (Liu et al., 2020). The average accuracies and standard deviations over five trials are reported. The best results sharing the noisy fraction and method are highlighted in bold.

Dataset	CIFAR-10				CIFAR-100			
Noisy Type	Sym		Asym		Sym		Asym	
Noise Ratio	40%	60%	80%	40%	40%	60%	80%	40%
Standard	81.9 \pm 0.3	74.1 \pm 0.6	53.8 \pm 1.0	80.1 \pm 1.4	48.2 \pm 0.7	37.4 \pm 0.9	18.1 \pm 0.8	42.7 \pm 0.6
ALASCA	90.9 \pm 0.1	86.2 \pm 0.2	72.7 \pm 0.6	91.2 \pm 0.1	67.2 \pm 0.2	56.8 \pm 0.5	31.0 \pm 0.4	65.1 \pm 0.5
GCE	87.1 \pm 0.2	82.5 \pm 0.2	64.1 \pm 1.4	76.7 \pm 0.6	61.8 \pm 0.2	53.2 \pm 0.8	29.2 \pm 0.7	47.2 \pm 1.2
GCE + ALASCA	90.4 \pm 0.2	87.0 \pm 0.2	76.2 \pm 0.7	88.5 \pm 0.2	67.7 \pm 0.1	60.5 \pm 0.3	32.2 \pm 0.5	57.3 \pm 0.5
SCE	87.1 \pm 0.3	82.8 \pm 0.6	68.1 \pm 0.8	82.5 \pm 0.5	62.3 \pm 0.2	54.8 \pm 0.6	25.9 \pm 0.4	48.4 \pm 0.9
SCE + ALASCA	91.0 \pm 0.2	87.0 \pm 0.3	75.4 \pm 0.5	87.5 \pm 0.4	69.6 \pm 0.2	60.9 \pm 0.2	35.1 \pm 0.3	59.2 \pm 0.6
ELR	89.2 \pm 0.2	86.1 \pm 0.5	73.9 \pm 0.6	90.1 \pm 0.5	68.3 \pm 0.3	59.3 \pm 0.7	29.8 \pm 0.6	73.3 \pm 0.6
ELR + ALASCA	91.1 \pm 0.2	88.0 \pm 0.3	77.2 \pm 0.4	91.3 \pm 0.4	69.7 \pm 0.2	62.6 \pm 0.3	34.3 \pm 0.4	73.6 \pm 0.4

Table 5. Test accuracies (%) on CIFAR-10 and CIFAR-100 under different noisy types and fractions for sample selection approaches. The average accuracies and standard deviations over five trials are reported.

Dataset	CIFAR-10				CIFAR-100			
Noisy Type	Sym		Asym		Sym		Asym	
Noise Ratio	40%	60%	80%	40%	40%	60%	80%	40%
Decoupling	85.9 \pm 0.4	81.3 \pm 0.2	44.3 \pm 1.4	85.9 \pm 0.9	59.7 \pm 0.3	45.9 \pm 0.3	17.7 \pm 0.9	59.6 \pm 1.7
A-Decoupling	88.4 \pm 0.2	82.7 \pm 0.3	60.6 \pm 1.0	87.8 \pm 0.7	65.5 \pm 0.4	47.8 \pm 0.2	21.4 \pm 1.3	66.9 \pm 0.7
Co-teaching	90.1 \pm 0.3	86.1 \pm 0.5	65.2 \pm 2.3	85.6 \pm 1.2	66.2 \pm 0.4	59.1 \pm 0.4	20.5 \pm 1.3	61.9 \pm 1.2
A-Co-teaching	92.0 \pm 0.2	88.7 \pm 0.3	70.7 \pm 0.7	91.2 \pm 0.8	71.5 \pm 0.3	63.7 \pm 0.5	25.6 \pm 1.2	70.8 \pm 0.6
CRUST	86.6 \pm 0.2	84.9 \pm 0.1	60.4 \pm 1.5	79.8 \pm 1.6	65.2 \pm 0.2	48.6 \pm 0.3	17.2 \pm 0.7	55.0 \pm 0.6
A-CRUST	90.5 \pm 0.1	86.2 \pm 0.2	70.8 \pm 0.5	88.8 \pm 0.5	67.3 \pm 0.3	57.0 \pm 0.2	24.8 \pm 0.5	66.1 \pm 0.4

Sample Selection Methods Sample selection which selects clean sample candidates from the whole training dataset is one of the most popular choices among the various methods for LNL. A widely used sample selection strategies for DNN training are to select with small training loss (Malach & Shalev-Shwartz, 2017; Han et al., 2018), or small weight gradient (Mirzasoleiman et al., 2020). In this section, we combine our proposed method with following sample selection approaches; (1) Decoupling (Malach & Shalev-Shwartz, 2017), (2) Co-teaching (Han et al., 2018), (3) CRUST (Mirzasoleiman et al., 2020). Table 5 summarizes the performances of different sample selection approaches on various noise distribution and datasets. We observe that our ALASCA method consistently improves the performance of networks compared to the network training with the naive sample selection method. Specifically, we experimentally show that the network trained robustly with ALASCA can select clean examples better than baseline in Figure 10, F-scores for A-Coteaching are consistently higher than original Co-teaching.

Semi-Supervised Approaches SSL approaches (Li et al., 2020; Liu et al., 2020) divide the training data into the clean and noisy as labeled and unlabeled examples, respectively, use both of them in semi-supervised learning. Recently, methods belonging to this category have shown the best performance among the various LNL methods, and these methods possibly train robust networks for even extremely high noise rates. However, pseudo labels generated from the corrupted networks might lead to the network as suboptimal. We combine the ALASCA with existing semi-supervised approaches and compare the performance with baseline. We achieve consistently higher performance than baseline since ALASCA enables robust training of feature extractor as shown in Table 6. Interestingly, as Figure 10 shows, clean and noisy data is well-divided in A-DivideMix under extreme noise case (CIFAR-10 with 90% symmetric noise).

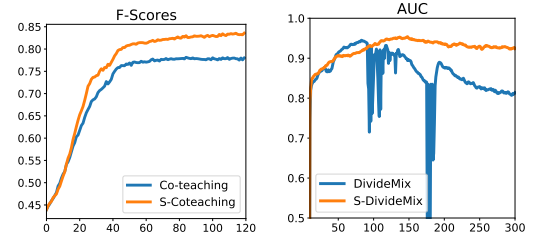


Figure 10. Comparison of F-scores on CIFAR-10 under 80% symmetric label noise (left) and comparison of AUC on CIFAR-10 under 90% symmetric label noise (right) along the training epochs. We experimentally show that robustly trained feature extractors through ALASCA select the high-quality subset consisting of (almost) clean examples.

Table 6. Comparison of test accuracies (%) for ALASCA collaborating with DivideMix (Li et al., 2020) and ELR+ (Liu et al., 2020) on CIFAR-10 and CIFAR-100 under different noisy types and fractions. The results for all comparison methods are taken from their original works.

Dataset		CIFAR-10					CIFAR-100				
Noisy Type		Sym			Asym		Sym			Asym	
Noise Ratio		20	50	80	90	40	20	50	80	90	40
DivideMix	Best	96.1	94.6	93.2	76.0	93.4	77.3	74.6	60.2	31.5	72.1
	Last	95.7	94.4	92.9	75.4	92.1	76.9	74.2	59.6	31.0	-
ELR+	Best	95.8	94.8	93.3	78.7	93.0	77.6	73.6	60.8	33.4	77.5
	Last	94.6	93.8	91.1	75.2	92.7	77.5	72.4	58.2	30.8	76.5
A-DivideMix	Best	96.3	95.3	93.7	79.4	93.5	77.5	75.1	61.8	32.7	72.4
	Last	96.0	95.0	93.4	78.5	92.8	77.1	74.8	60.6	32.2	71.8
A-ELR+	Best	96.1	95.0	93.6	78.7	94.0	77.9	74.0	61.0	34.8	78.1
	Last	95.6	94.8	92.8	78.1	93.2	77.9	73.7	59.6	34.3	77.3

Table 7. Test accuracies (%) on CIFAR-10 and CIFAR-100 under different types and fractions for regularization methods. For HAR (Cao et al., 2020) and CDR (Xia et al., 2020), we apply their official code. The average accuracies and standard deviation over five trials are reported. The best and second-best results sharing the noisy fraction (or same efficiency criterion) are highlighted in bold and underline.

Dataset	CIFAR-10				CIFAR-100				Efficiency	
	Sym		Asym		Sym		Asym		Mem.	Time
Noise Ratio	40%	60%	40%	40%	40%	60%	40%	40%	(GiB/GPU)	(sec/step)
Standard	81.9 ± 0.3	74.1 ± 0.6	80.1 ± 1.4	75.2 ± 2.1	48.2 ± 0.7	37.4 ± 0.9	42.7 ± 0.6	41.1 ± 1.2	-	-
Mixup	88.2 ± 0.2	84.2 ± 0.2	89.1 ± 0.2	83.1 ± 1.2	63.1 ± 0.2	54.6 ± 0.4	62.1 ± 0.5	51.6 ± 0.9	× 1.0	× 1.0
HAR	88.6 ± 0.1	83.6 ± 0.3	89.0 ± 0.2	83.5 ± 0.8	54.4 ± 0.3	42.8 ± 0.5	49.7 ± 1.0	45.4 ± 1.5	× 2.0	× 5.2
CDR	87.0 ± 0.2	80.1 ± 0.5	<u>89.5 ± 0.3</u>	82.8 ± 0.6	60.5 ± 0.5	51.8 ± 0.7	52.2 ± 0.7	48.7 ± 0.8	× 1.3	× 6.5
ALASCA	90.9 ± 0.1	86.2 ± 0.2	91.2 ± 0.1	84.7 ± 0.4	67.2 ± 0.2	56.8 ± 0.5	65.1 ± 0.5	53.4 ± 0.7	× <u>1.1</u>	× <u>1.2</u>

D.3. Additional Results

D.3.1. COMPARISON WITH EXISTING REGULARIZATION METHODS

To verify our implicit regularization framework ALASCA, we compare its performance of ALASCA with standard training and existing regularization methods. We compare our framework with the following regularization-based approaches: (1) (uniform) LSR (Lukasik et al., 2020): it modify each one-hot label to smooth label with $\alpha = 0.5$, (2) Mixup (Zhang et al., 2017b): it trains network on convex combinations of pairs of examples and their labels, (3) HAR (Cao et al., 2020): it explicitly and adaptively regularizes the norm of Jacobian matrices of the data points in higher-uncertainty, lower-density regions more heavily, (4) CDR (Xia et al., 2020): it identify and regularize the non-critical parameters which tend to fit noisy labels and cannot generalize well. While the latter two methods are similar to our proposed method to regularize the intermediate layer; however, they are explicit regularization methods that find noise data points or non-critical parameters to regularize them. Table 7 provides the performance of different regularization-based methods on various noise distribution and datasets. For the efficiency test, since the training stages for each method are different, we compute the computation memory and training time with entire training procedure.² We observe that our ALASCA method consistently outperforms the competitive regularization-based methods over the various noise types and rates as well as enables effective training in terms of computation memory and training time.

D.3.2. ROBUST TO HYPERPARAMETERS SELECTION OF LNL METHODS

Existing LNL methods have significant performance differences depending on their hyperparameters, and if we select hyperparameters value improperly, the performance is provably lower than of standard training. However, the values of the optimal hyperparameters vary depending on the network architectures or datasets. Despite its importance, many works do not focus on hyperparameter selection, and it is challenging to achieve performance improvement in real-world datasets, as reported in the original work. We combine the ALASCA and existing LNL method with various hyperparameter settings: (1) Standard training with different weight decay coefficients (2) ELR (Liu et al., 2020) with different regularization coefficient

²For example, HAR needs to train network twice to estimate regularization power and train with regularization for the re-initialized network. CDR needs to additional computation to identify non-critical parameters.

(3) Co-teaching (Han et al., 2018) along the different warmup epochs (4) CRUST (Mirzasoleiman et al., 2020) with different coreset sizes. The detailed experimental setups are as follows:

Standard Training. Yu et al. (Yu et al., 2019) argue that LSR denoise label noise by encouraging weight shrinkage of DNNs. Motivated by this view, we find that the performance of network are varying depends on weight decay factor for training. We train the networks with weight decay factor of $1e-4$ (S1), $5e-4$ (S2), and $1e-3$ (S3).

Early Learning Regularization. ELR (Liu et al., 2020) uses two types of hyperparameters: the temporal ensembling parameter β and the regularization coefficient λ . They perform hyperparameter tuning on the CIFAR datasets via grid search. The selected values are $\beta = 0.7$ and $\lambda = 3$ (S1) for CIFAR-10 with symmetric noise, $\beta = 0.9$ and $\lambda = 1$ (S2) for CIFAR-10 with asymmetric noise, and $\beta = 0.9$ and $\lambda = 7$ (S3) for CIFAR-100. We train the network with CIFAR-10 under 40% asymmetric noise with hyperparameter settings S1, S2, and S3.

Co-teaching. The warm-up epochs for Co-teaching (Han et al., 2018) is very important. If number of warm-up epochs is too small, the network start to filter the noisy examples with underfitted network parameters to clean examples while the network is overfitted to noisy examples if number of warm-up epochs it too large. While the original paper reports the warm-up epochs as 30, here, we train the network with warm-up epochs 10 (S1), 20 (S2), 30 (S3).

CRUST. The coreset size is important to CRUST since the network risks overfitting to noisy examples with large coreset and underfitting to clean examples with small coreset. The original paper of CRUST (Mirzasoleiman et al., 2020) select the coresets of size 50% of the size of the dataset. In our experiments, we train the networks with coreset size of 30% (S1), 50% (S2), 70% (S3) of the size of the dataset.

The results are shown in Table 8. Since the optimal hyperparameters vary depending on the experiment settings, we conduct the experiments on various network and noise rate. While the baseline performances broadly differ depending on the hyperparameter settings, performances with ALASCA sustain robustly even when different hyperparameters are used.

D.3.3. COMPONENTS ANALYSIS

We perform an analysis on each component of our method, namely the use of EMA confidence (EMAC) and label correction with agreement (LCA), by comparing their test accuracy. Our experiments are conducted on CIFAR10 under various noise distribution. The results in Table 9 demonstrate each component is indeed effective, as the performance improves step by step with the addition of the component.

Table 8. Comparison of test accuracies (%) along the different hyperparameter settings for various LNL methods. Note that the first and second rows for each experiment set are corresponding to without and with ALASCA, respectively.

Method	Network	Dataset	Hyperparameter		
			S1	S2	S3
CRUST (coreset size)	WRN28-4	CIFAR-10 Sym 20%	81.14 91.96	83.12 91.04	89.86 91.20
Standard (WD)	VGG19	CIFAR-10 Sym 60%	72.92 79.07	77.67 80.69	80.05 81.53
Co-teaching (warmup)	ResNet32	CIFAR-10 Sym 80%	25.96 49.57	31.80 51.01	43.08 50.04
ELR (λ, β)	PreAct- ResNet18	CIFAR-10 Asym 40%	83.27 87.87	86.75 89.23	89.72 90.91

Table 9. Ablation study on each component of our proposed learning framework. The bold indicates the best result.

	Sym 40	Sym 60	Sym 80	Asym 40
ALS (S)	88.4	82.6	69.2	88.5
+ EMAC	89.7	84.8	70.4	90.2
+ LCA	89.5	85.1	71.0	89.8
ALASCA	90.9	86.2	72.7	91.2